CHEMISTRY OF MATERIALS

ARTICLE

pubs.acs.org/cm

Mesostructures of Polyaniline Films Affect Polyelectrochromic Switching

Jacob Tarver* and Yueh-Lin Loo*

Department of Chemical and Biological Engineering, Princeton University, Princeton, New Jersey 08544, United States

ABSTRACT: The dynamics of polyelectrochromic switching in films of polymer-acid-doped polyaniline (PANI) having different internal film structures — and thus different extents of exposed surface area — was investigated. We present a simple model that captures the influence of PANI's mesostructure on its transitions between the insulting and conducting states. Films possessing high internal surface areas exhibit longer electrochromic switching times relative to films with low exposed surface areas. By homogenizing the mesostructures via solvent-induced structural relaxation of PANI thin films, the polyelectrochromic response of PANI hastens and differences are eliminated. This solvent-induced structural relaxation effectively increases the extent of percolation of conductive pathways, resulting in shorter electrochromic switching times as PANI transitions from insulating to conductive states. Increasing the size of the buffer cation also results in longer switching times in mesoscopically heterogeneous films. Following structural relaxation and homogenization, the influence of the buffer cation on polyelectrochromic switching kinetics is eliminated. These correlations point to the importance of internal film structure in electrochromic switching of conducting polymers, and provide insights for the design of next-generation electrochromic polymer systems.

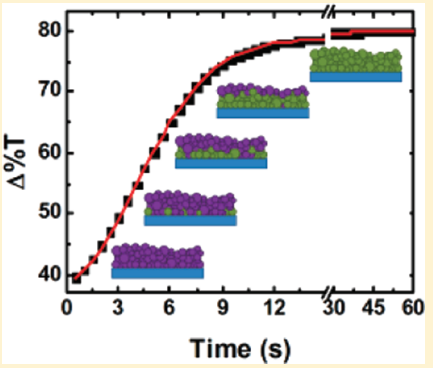

KEYWORDS: polyaniline, electrochromic thin films, conducting polymers, switching, redox

Electrochromism characterizes a material's ability to undergo reversible changes in its optical properties upon the addition or withdrawal of charge. Films comprising electrochromically active species can be manipulated to moderate their transmitted or reflected spectrum of incident light. Application of a characteristic oxidation potential, for instance, can render a transparent electrochromic film dark and opaque, while application of a corresponding reduction potential can return the film to its initial state.[1] Electrochromic materials have thus been proposed as active components in smart windows that are capable of adjusting the level of tinting as-desired, or in response to changing daylight intensity.[2] Devices comprising electrochromic materials have also been put forth as promising components in externally lit large-area displays due to their low power consumption; reversible and persistent color changes can be effected by short pulses of current without a continuous supply of power, as opposed to the constant load of current required for sustained emission in light emitting diodes (LEDs).[3]

π-conjugated polymers have proven to be superb candidates for next-generation electrochromic materials. The rich redox chemistry imbued by the backbones of conjugated polymers, such as polythiophene and polypyrrole, and the ability to tune the optical band gap through simple chemical derivatization and copolymerization, provide the foundation for exploring the enormous electrochromic potential of these materials.[4] In addition to tailored optical properties, π-conjugated polymers often behave as electrical conductors or semiconductors in their oxidized forms, and have therefore been heavily utilized in other fields of organic electronics.[5−7] The relationship between the molecular structure and optical properties of electrochromic polymers has received much attention, as seen by the rapid increase in the array of electrochromic polymers available in recent years. By varying the side-chain chemistry of various monomer derivatives, and by manipulating their subsequent copolymerization conditions, vast libraries of electrochromic and polyelectrochromic polymer systems synthesized by Reynolds and others can readily switch between their transparent, electrochemically reduced states and their colored, electrochemically oxidized states spanning the entire visible range.[8−13]

Polyaniline (PANI) is a unique conjugated polymer that, unlike systems comprising thiophenes and pyrroles, is capable of multiple electrochromic transitions in its homopolymer form, thus obviating the need for additional chemical derivatization or copolymerization.[14] In its fully reduced form, known as leucoemeraldine base (LB), PANI is transparent and electrically insulating; in its fully oxidized form, known as pernigraniline base (PB), PANI is violet and also electrically insulating. A stable proton-doped intermediate state, emeraldine salt (ES), exists between these two extremes. This green form of PANI exhibits significant electrical conductivity, and has been the subject of active research for the past few decades.[15−18]

Although intrinsically capable of polyelectrochromism, a number of limitations have prevented researchers from exploiting PANI's potential for exhibiting multiple colored states. While electrochemically grown PANI films doped with small-molecule

Received: August 8, 2011
Revised: August 29, 2011
Published: September 12, 2011

Scheme 1. Reaction Sequence Showing Transitions Between (a) Fully Reduced LB, (b) Partially Oxidized ES, and (c) Fully Oxidized PB[a]

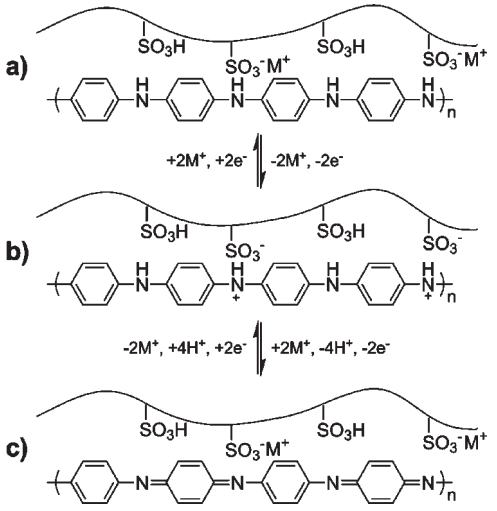

[a] M^+ initially represents PAAMPSA's protons, but on subsequent cycling in electrolyte solutions can represent other monovalent cation.

acids that are cycled in moderate-to-highly acidic electrolytes have shown excellent switching between the ES and LB states;[19] switching between ES and PB states, however, requires voltages that exceed the stable limits of PANI and in turn induces polymer degradation.[20] Increasing the pH can reduce the potential that is required for ES/PB switching to occur, but this change leads to a net efflux of ES's small molecule dopants upon switching to LB or PB and, accordingly, an eventual loss of electroactivity. This chemical degradation is reported to occur below pH 3, at which the redox potential to sustain reversible transitions between ES/PB remains inaccessible.[21]

Several strategies have been proposed to overcome the difficulties experienced with small-molecule acid dopants. Layer-by-layer assembly methods, for example, employ polymer acids as dopants; their high molecular weights prevent diffusion away from the conducting polymer upon transitioning away from ES, thereby overcoming the inherent pH restrictions imposed by small-molecule acid dopants.[22] However, even the highest performance films produced via this technique exhibit slow electrochemical transitions in comparison to small-molecule-doped PANI, presumably due to mass transfer limitations of ions through compact interlayers of PANI and its polymer acid dopant.[23] Other efforts to generate films incorporating polymer acid dopants either by electropolymerization or by chemical bath deposition during oxidative polymerization have shown to improve the switching window and retention of electroactivity at elevated pH's, but these materials still suffer from prohibitively slow switching speeds (1×10^1 to 1×10^2 s).[24,25]

An alternative method of producing polyelectrochromically viable PANI is its template synthesis directly on polymer acid dopants. Synthesis of PANI in the presence of poly(2-acrylamido-2-methyl-1-propanesulfonic acid), or PAAMPSA, yields water-dispersible PANI-PAAMPSA particles,[26,27] the size and size distribution of which depends on PAAMPSA's molecular weight and molecular weight distribution.[28] Films comprising PANI-PAAMPSA particles can be quickly and easily spun cast from aqueous dispersions; these films exhibit stable and reversible switching between PANI's LB, ES, and PB oxidation states (Scheme 1). With PANI-PAAMPSA films, we can access all three oxidative forms within a potential window of 0.9 to −0.5 V (vs Ag/AgCl) while maintaining switching times on the order of 10^0-10^1 s.[29,30] Recently, we discovered that solvent annealing PANI-PAAMPSA films in dichloroacetic acid (DCA) induces strong structural rearrangement that in turn alters the films' electrochromic properties.[29,31] Specifically, this treatment significantly increases the rate and the extent of electrochromic transitions while simultaneously conferring enhanced reversibility to switching.[29,31]

Comparison between the electrochromic performance of PANI and other conjugated polymers is complicated by a lack of systematized parameters quantifying the kinetics of color switching. Often, researchers merely cite the time that is required to achieve an arbitrary metric, such as 90−95% of total induced contrast, to quantify switching kinetics.[32,33] In one specific case, the electrochromic kinetics of PANI's ES/LB transition were modeled and fitted. The researchers found a linear combination of two simple exponential functions to fit the data well, implying that the transition is dominated by two separate processes.[25] The faster process was found to dominate the initial electrochromic response of the film, and was attributed to the rapid reaction of a connected network of PANI clusters forming a percolated conduction path directly to the electrode. The second process was found to describe the electrochromic response at longer time scales and was attributed to the gradual reaction of residual, electrically isolated PANI clusters. Although simplistic in approach, this model provided acceptable agreement with PANI's switching response. More importantly, it implicated the influence of mesoscale structure via percolated conduction pathways on the electrochromic kinetics of conjugated polymers. Despite significant progress in understanding how the molecular structure of these materials can be modified to tune their electrochromic color range, there has been little investigation toward identifying how the mesoscopic structure influences their electrochromic switching kinetics.

We have previously demonstrated the ability to tune the size and size distribution of particles comprising our electrochromic polymer by controlling the molecular weight and molecular weight distribution of the PAAMPSA template, respectively. Assuming a constant macroscopic packing fraction of PANI-PAAMPSA particles, as supported by simulations,[28] control over the size and size distribution of PANI-PAAMPSA particles provides tunability over the mesoscopic structure of the cast films as quantified by the particle surface area per unit film volume, A_i/V. The ability to controllably vary A_i/V provides, for the first time, an opportunity to quantify how systematic variations in the mesoscale structure of PANI-PAAMPSA films influence electrochromic kinetics. By eliminating variations in the films' mesoscale structure via DCA-induced structural relaxation, we subsequently demonstrate the elimination of variations in PANI-PAAMPSA's electrochromic response. Additionally, we show that as-spun PANI-PAAMPSA exhibits a direct correlation between electrochromic switching time and electrolyte cation size. Following DCA treatment, during which the mesoscopic structure is relaxed, however, this effect is eliminated. Rather than employing the dual-simple-exponential model described above, we find a linear combination of simple and stretched exponentials to best describe the kinetics of transformation in our PANI-PAAMPSA films. Quantification of

the relevant kinetic parameters in our model allows differentiation between ES/LB, ES/PB, and LB/PB transitions, and provides distinction between as-spun and DCA-treated films, with the model shedding light on how these different transitions occur.

EXPERIMENTAL SECTION

Polyaniline was template synthesized on PAAMPSA as described by Yoo et al.[26] Commercially available PAAMPSA (10.36 wt % in water, Polymer Supply, Inc.), possessing a poly(ethylene oxide) (PEO) equivalent molecular weight of 724 kg·mol^{-1} and a PDI of 1.64, was used as-purchased to template synthesize PANI-PAAMPSA-724; the resulting conducting polymer complex forms particles with average hydrodynamic diameters of 1232 ± 25 nm that can be precipitated for storage and resuspended in water to yield the same particle size distribution.[28] Two PAAMPSA templates possessing lower molecular weight (150 and 287 kg mol^{-1}) and narrower PDI (1.25 and 1.28, respectively) were synthesized in-house via atom transfer radical polymerization (ATRP) and employed to generate PANI-PAAMPSA having smaller particle sizes and narrower size distributions (782 ± 18 and 820 ± 16 nm, respectively).[27,28] To differentiate these samples from PANI-PAAMPSA-724, they are referred to as PANI-aPAAMPSA-150 and PANI-aPAAMPSA-287, respectively, where aPAAMPSA denotes PAAMPSA that was derived through ATRP and the numbers denote the molecular weight of aPAAMPSA, in kg/mol.

Precleaned indium tin oxide (ITO, 15 Ω/□, Colorado Concept Coatings) on glass was used as an optically transparent working electrode during spectral characterization. To promote PANI-PAAMPSA adhesion upon deposition, and to prevent film delamination during electrochromic studies in buffer solutions, the surface of ITO was first treated with 12-phosphonododecylphosphonic acid (97%, Sigma Aldrich) using the tethering-by-aggregation-and-growth (T-BAG) method.[34] The bisphosphonic acid was dissolved in an anhydrous mixture of 95% tetrahydrofuran/5% methanol at 0.1 mM concentrations into which ITO substrates were suspended. The solution was then allowed to evaporate, resulting in the covalent attachment of the bisphosphonic acid to ITO at the air/solution interface via condensation chemistry with ITO's surface-bound hydroxyl groups. Following deposition, the substrates were baked at 130 °C for 24 h to drive the condensation reaction to completion. After the substrates were successively sonicated for 10 min in water, acetone, and isopropanol to remove physisorbed bisphosphonic acid, PANI-PAAMPSA was spun-cast from 5 wt % aqueous dispersions to yield films having a nominal thickness of 450 nm, as measured with a Dektak 3.21 profilometer. All films were dried at 100 °C for 2 min prior to use.

To induce structural relaxation of PANI-PAAMPSA films, we performed solvent annealing in DCA as described by Yoo et al.[31] PANI-PAAMPSA films were immersed in DCA at 100 °C and vigorously agitated for 3 min. These films were then heated at 170 °C for 30 min to remove residual DCA. Following DCA treatment, the films densified to a nominal thickness of 300 nm.

Electrochemistry was performed in pH 5.0 100 mM acetate buffer solutions comprising glacial acetic acid (100.0%, Fisher Scientific) and one of the following alkali metal acetate salts: lithium acetate dihydrate (98%, Acros Organics), anhydrous sodium acetate (99%, EMD Chemicals), or potassium acetate (99.8%, Fisher Scientific). All water was purified to 18.2 MΩ prior to use with a Milli-Q Academic purification system.

Electrochromic experiments were carried out in a 1.2 mL PTFE spectroelectrochemical cell featuring a 1 cm diameter optical port. Time-resolved spectral characterization was performed across a wavelength range of 300−1100 nm using an Agilent 8453 spectrophotometer with 1 nm spectral resolution and 0.5 s temporal resolution; clean ITO substrates were used as background. Potential step measurements were performed with a CH-Instruments 660C potentiostat in a three-electrode configuration employing a platinum wire counter electrode and a Ag/AgCl reference electrode.

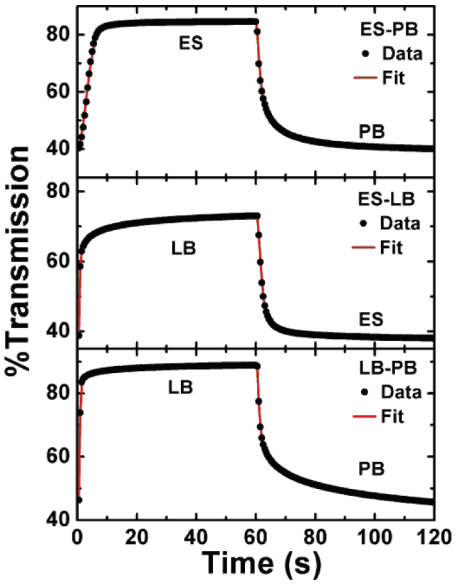

Figure 1. UV−vis transmission response of as-spun PANI-PAAMPSA undergoing transitions between the ES and PB oxidations states (top), the LB and ES oxidation states (middle), and the LB and PB oxidation states (bottom). Traces are reported (●) and fitted (red line) at the wavelength associated with maximum contrast. Switching was performed in 100 mM pH 5 sodium acetate buffer.

RESULTS AND DISCUSSION

Figure 1 shows UV−vis transmission responses recorded for ES/PB, ES/LB, and LB/PB transitions for as-spun PANI-PAAMPSA-724 films. The optical response was measured while stepping the applied potential between previously identified potential limits of 0.9 V for PB, 0.2 V for ES, and −0.5 V for LB.[29] The films were held at each potential step for 60 s, and the full 120 s cycle was repeated at least 10 times for transitions between each binary combination of the three oxidation states. Each transition approaches completion within the first 10 s of switching the applied potential. A large degree of variation, however, can be observed in PANI-PAAMPSA's response during the initial portion of each cycle. We found that the kinetics observed when switching PANI-PAAMPSA-724 from one oxidation state to another upon application of a corresponding potential can be quantitatively described by a combination of two exponential terms, as shown in eq 1 below, suggesting two additive processes taking place

$$\Delta\%T = \%T_o \pm A_1[1 - \exp(-t/\tau)] \pm A_2[1 - \exp(-kt^n)] \quad (1)$$

In eq 1, $\%T$ represents the percent transmitted light at the wavelength of maximum contrast recorded for the transition; A_1 and A_2 represent scaling constants for each exponential term; τ represents the time constant for the simple exponential term; k and n represent the time constant and exponent, respectively, for the stretched exponential term, and t represents time.

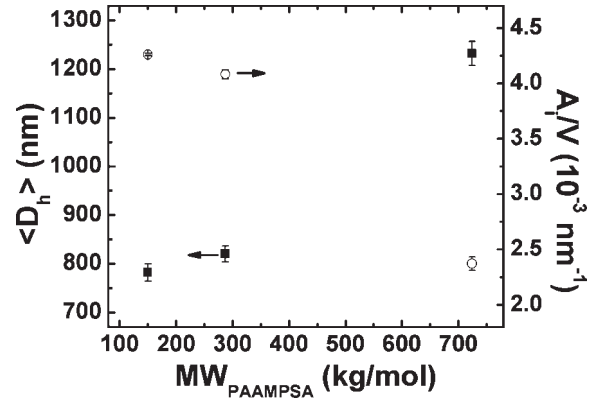

Figure 2. Structure of PANI-PAAMPSA as quantified by the hydrodynamic diameter of particles prior to casting (■, $\langle D_h \rangle$) and surface area per unit volume of thin films (○, A_i/V) as a function of molecular weight PAAMPSA for PANI-aPAAMPSA-150, PANI-aPAAMPSA-287, and PANI-PAAMPSA-724.

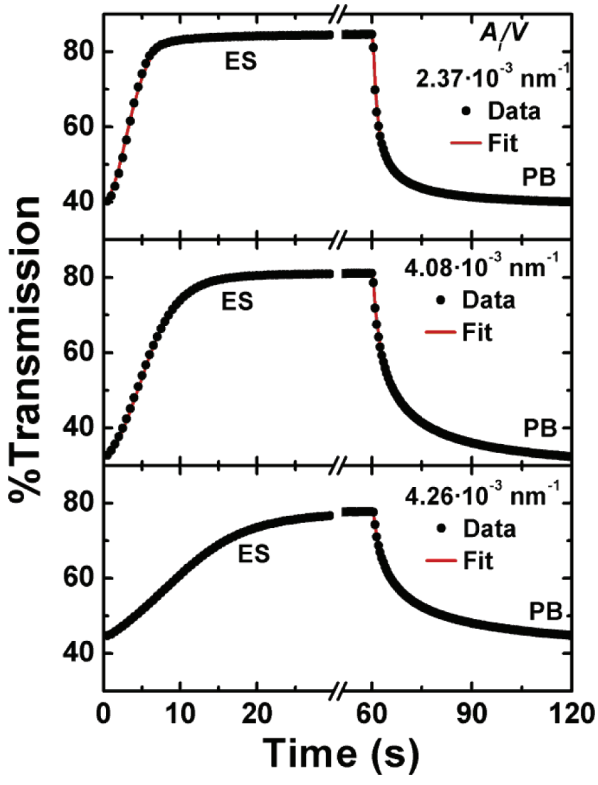

Figure 3. UV−vis transmission response of as-spun PANI-PAAMPSA-724 (top), PANI-aPAAMPSA-287 (middle), and PANI-aPAAMPSA-150 (bottom) films while undergoing transitions between the ES and PB oxidation states. The average internal surface area per unit film volume is reported in the legend of each transmission plot. Switching was performed in 100 mM pH 5 sodium acetate buffer. Traces are reported (●) and fitted (red line) at the wavelength associated with maximum contrast.

We have previously shown that the internal mesoscale structure of PANI-PAAMPSA thin films depend on particle size, which we can tune at the onset of synthesis by varying the PAAMPSA template molecular weight.[28] Quantification of the particle size and size distribution by dynamic light scattering has allowed us to extract A_i/V of PANI-PAAMPSA, effectively quantifying the internal mesoscale structure in these thin films. Figure 2 simultaneously plots the average particle size and A_i/V for the three conducting polymers examined in this study against their template molecular weights. We can access a range of particle size, and accordingly A_i/V, simply by varying the molecular weight of the PAAMPSA template at the onset of synthesis. Previous work has established that the electrical conductivity of PANI-PAAMPSA thin films scales superlinearly with A_i/V, suggesting that the conductive portions of PANI-PAAMPSA — unlike that of the more common poly(ethylene dioxythiophene) that is doped with poly(styrene sulfonate), or PEDOT-PSS[35] — are predominately segregated to the surface of the particles.[28] Given the influence of A_i/V on PANI-PAAMPSA's charge transport characteristics in the solid state, we hypothesize that this quantity, a direct measure of the mesoscale structure of PANI-PAAMPSA thin films, should influence the dynamics of PANI-PAAMPSA's electrochromic properties as well. The ability to tune PANI-PAAMPSA's internal structure thus provides an opportunity to explore how such differences affects transformation kinetics. The transmission responses for PANI-aPAAMPSA-150, PANI-aPAAMPSA-287, and PANI-PAAMPSA-724 as they are throttled from the ES to PB states are shown in Figure 3.

During data fitting of the transmission responses of PANI-PAAMPSA-724 in Figure 1 to eq 1, the time constant associated with the first-order exponential function, τ, was initially allowed to float. We quickly observed, however, that this parameter consistently settled near 15 s for all transitions regardless of buffer strength across a range of 0.01 to 1.0 M. Additionally, step durations below 60 s do not alter τ; only by extending step durations beyond 60 s do we observe a demand for proportional increases in τ to yield adequate data fits. Further, τ appears to maintain near 15 s for PANI-aPAAMPSA-150 and PANI-aPAAMPSA-287, each having different internal film structures. Given our experimental observations, we surmise that the slow drift in $\%T$ that we ascribe to the simple exponent must stem from our experimental setup and its origin beyond the scope of this present study as it does not appear to pertain to the influence of structure on the electrochromic switching characteristics of PANI-PAAMPSA. For simplicity, we have thus held τ constant at 15 s throughout our analysis.

In fitting our data in Figure 1 to eq 1 above, we observe that transitions to the electrically insulating LB and PB states are best described by $n = 1.5$. Transitions to the electrically conducting ES state of as-spun PANI-PAAMPSA-724, alternatively, are best described by $n = 2$, regardless of whether the film is initially in the LB or PB state. Our model provides quantitative agreement with our data in each scenario. In particular, the inclusion of the stretched exponential function in eq 1 allows us to account for the unusual sigmoidal character observed for the film's PB to ES transition. This sigmoidal characteristic of PANI's electrochromic response as it transitions from PB to ES is more apparent in PANI-aPAAMPSA-287 and PANI-aPAAMPSA-150 films; the responses of which are shown in Figure 3. This feature has not previously been reported in experiments focused only on the purely electronic LB to ES transition, and as a consequence, has been beyond the scope of previous kinetic models.[25] Although less pronounced in PANI-PAAMPSA's LB to ES transition relative to that of PB to ES, the sigmoidal functionality imposed by a value of $n = 2$ provides superior agreement with experimental data for both reactions. That this behavior has not

previously been reported in PANI's switching kinetics is likely due to the inability of the systems under study in the past to reversibly access the PB state without imposing significant chemical degradation. We speculate that the pronounced sigmoidal character clearly observed in the PB to ES transition stems from the reaction's additional reliance on the influx of protons (see Scheme 1 for chemical reaction), further limiting the time-scale of the transition. We thus propose that this stretched exponential term is associated with the nucleation and auto-accelerated propagation of conductive pathways away from the electrode surface as PANI-PAAMPSA is throttled from an insulating oxidation state to a potential that readily renders it conductive. At the onset of the transition to the conductive ES state, the film is uniformly in its insulating PB state, and as a consequence, the applied potential and ensuing electrochemical reactions are limited to a region near the ITO/PANI-PAAMPSA interface. As portions of PANI-PAAMPSA near the ITO electrode are reduced to the conductive ES state, local ohmic losses are reduced, and the applied potential can extend further into the film; these conductive ES portions can in turn transport charge to induce the subsequent reaction of material deeper within the film in a manner analogous to the Avrami kinetics commonly used to describe polymer crystallization.[36−38] Drawing further analogies to the Avrami kinetics of crystallization, we infer that the value of n extracted from the kinetics of transitions from LB or PB to the ES state for as-spun PANI-PAAMPSA reflects two-dimensional propagation of the reaction front along film depth with nucleation of the reaction occurring instantaneously at the ITO surface as the appropriate potential is applied.[36−38]

To assess the influence of mesoscale structure on the nature of the PB to ES transition, and its impact on the propagation of percolated conduction pathways, we explored the dynamics of electrochemically induced transitions of PANI-PAAMPSA having different A_i/V. Figure 3 tracks the % transmission during the electrochromic switching between the ES and PB states of films comprising PANI-aPAAMPSA-150, PANI-aPAAMPSA-287, and PANI-PAAMPSA-724 particles under conditions identical to those used to obtain the results shown in the top panel of Figure 1. These particles possess average hydrodynamic diameters, $\langle D_h \rangle$, of 782, 820, and 1230 nm, which in turn lead to A_i/V of 4.26×10^{-3}, 4.08×10^{-3}, and 2.37×10^{-3} nm^{-1}, respectively. We can quantify the rate at which this process takes place by extracting the halftime, $t_{1/2}$, of the stretched exponential term in eq 1. Our picture of two-dimensional propagation of the reaction front as PANI-PAAMPSA is throttled between its insulating and conducting states mandates that this parameter should hinge on the internal structure of PANI-PAAMPSA thin films. Indeed, comparison of the electrochromic response of these films reveals drastic differences in the switching times, with PANI-PAAMPSA-724, the thin film having the lowest A_i/V, exhibiting the shortest switching times.

Quantification of $t_{1/2}$ reveals systematic but large variations as the films are switched from PB to ES states. In particular, PANI-PAAMPSA-724 exhibits $t_{1/2}$ = 3.5 s and approaches its terminal ES form within 10 s. PANI-aPAAMPSA-287 and -150, alternatively, exhibit $t_{1/2}$ = 5.5 and 10.3 s, respectively, and require in-excess-of 20 s to transition from PB to ES. In consideration of our electrochromic kinetic model, the trends extracted from the data depicted in Figures 2 and 3 collectively suggest that the increased A_i/V in PANI-PAAMPSA thin films requires longer switching times for the same electrochromic transition to take place due to a slowing down in the propagation of percolated conduction

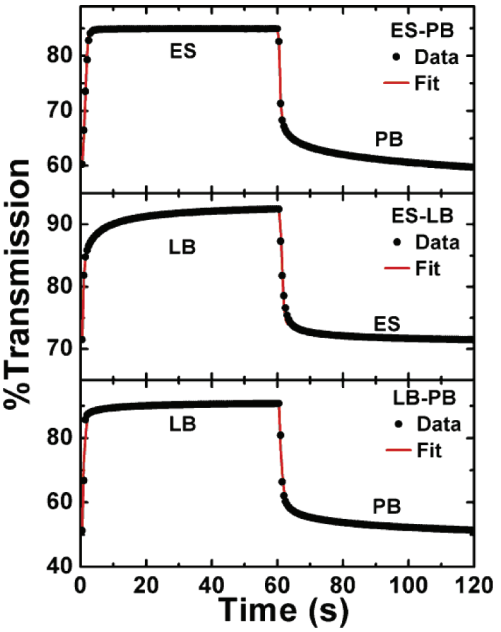

Figure 4. UV−vis transmission response of DCA-treated PANI-PAAMPSA undergoing transitions between the ES and PB oxidations states (top), the LB and ES oxidation states (middle), and the LB and PB oxidation states (bottom). Traces are reported (●) and fitted (red line) at the wavelength associated with maximum contrast. Switching was performed in 100 mM pH 5 sodium acetate buffer.

pathways. We thus surmise that interparticle contacts are bottlenecks for the electrochromic reactions that convert insulating PANI to its conductive state. These results were initially surprising in light of our previous research showing that macroscopic electrical conductivity correlates superlinearly with A_i/V.[28] The two scenarios in question, however, are fundamentally different in that charge transport across a uniformly conductive film is scrutinized in the former case whereas the rate of reaction as the film is converted into its conductive state is examined in the present case. Collectively, our results thus indicate that while interparticle contacts at high A_i/V limit PANI's transition from its insulating to conductive forms, these very same contacts actually promote solid-state charge transport once the entire film is converted to ES. It is worth noting that although $t_{1/2}$ varies dramatically across the specimens examined, n maintains a value of 2 for all three films. This observation indicates that the mechanism by which conductive pathways percolate through PANI-PAAMPSA is comparable among these films.

Solvent annealing with DCA can catalyze dramatic structural rearrangements of PANI-PAAMPSA films by moderating the electrostatic interactions binding PANI to PAAMPSA, and subsequently plasticizing and relaxing the high-molecular-weight PAAMPSA chains.[31] Following DCA-induced structural relaxation, variations in the electrical conductivity of PANI-PAAMPSA films that arise from differences in particle size and size distribution are eliminated; this observation suggests that the internal structure of PANI-PAAMPSA films is homogenized following DCA treatment, regardless of their previously disparate qualities. To determine the influence of this structural relaxation on PANI-PAAMPSA's polyelectrochromic kinetics, we also assessed the optical response of films after DCA treatment under conditions that are identical to those of as-spun films (Figure 4). The electrochromic transitions to each of PANI's oxidation

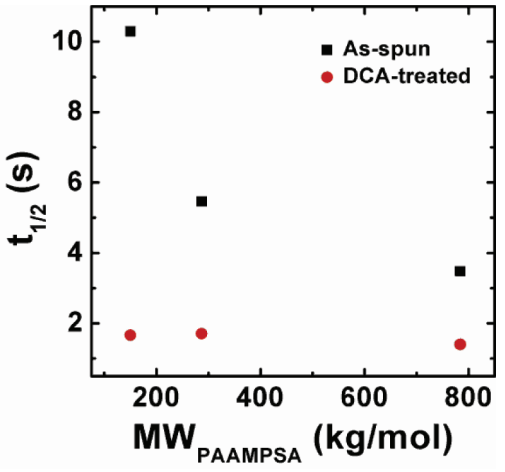

Figure 5. Extracted halftimes for PB to ES transitions as a function of PAAMPSA molecular weight for (black square) as-spun and (red circle) DCA-treated PANI-PAAMPSA.

states are greatly hastened and stabilized, as described in previous reports.[29] Fitting the data to eq 1 yields the same time constant associated with the simple exponential term, τ, of 15 s and indicates its invariance to DCA treatment. This observation further supports our assignment of the simple exponential term to our experimental setup. Also in agreement with the switching kinetics observed in as-spun films, transitions to the LB and PB states are best described by $n = 1.5$ for all PANI-PAAMPSA films post-DCA treatment. Unlike the switching kinetics observed in as-spun films, however, transitions to the electrically conductive ES state of DCA-treated PANI-PAAMPSA are best described by $n = 3$. That the exponents associated with this process differ between as-spun and DCA-treated PANI-PAAMPSA films emphasizes differences in the dimensionality of percolation of conductive pathways.

The higher value of n attributed to ES transitions in DCA-treated films ($n = 3$), accordingly, suggests three-dimensional propagation of the developing conductive phase through a dense film in which the particles have collapsed and homogenized.

We observe the transition from PB to ES states in DCA-treated films to be significantly faster than those of as-spun PANI-PAAMPSA films. Since it no longer makes sense to describe these films in terms of A_i/V following DCA treatment, extracted halftimes are shown in Figure 5 as a function of PAAMPSA molecular weight on which all three PANI-PAAMPSA were synthesized before and after DCA treatment. Quantification per fitting the data to eq 1 reveals comparable halftimes for all three DCA-treated films ($t_{1/2} = 1.4$, 1.7, and 1.7 s, respectively). Accordingly, we surmise that differences in the kinetics of PANI-PAAMPSA films prior to DCA treatment must be a direct manifestation of differences in their mesoscopic structure. The structural rearrangement induced by DCA treatment homogenizes the internal structure of PANI-PAAMPSA films, effectively removes particle-particle contacts that limit the propagation of reaction, and consequently, hastens the kinetics and eliminates variations associated with their electrochromic response.

To further assess the influence of film structure on the PB to ES transition for as-spun and DCA-treated PANI-PAAMPSA, we conducted electrochromic cycling in a series of pH 5, 100 mM acetate buffer solutions comprising acetic acid and lithium, sodium, or potassium acetate. In this manner, we were able to employ variations in cation size as probes of the role nanoscopic structure plays in electrochromic kinetics while effectively maintaining all other properties associated with the buffer and the PANI-PAAMPSA films.

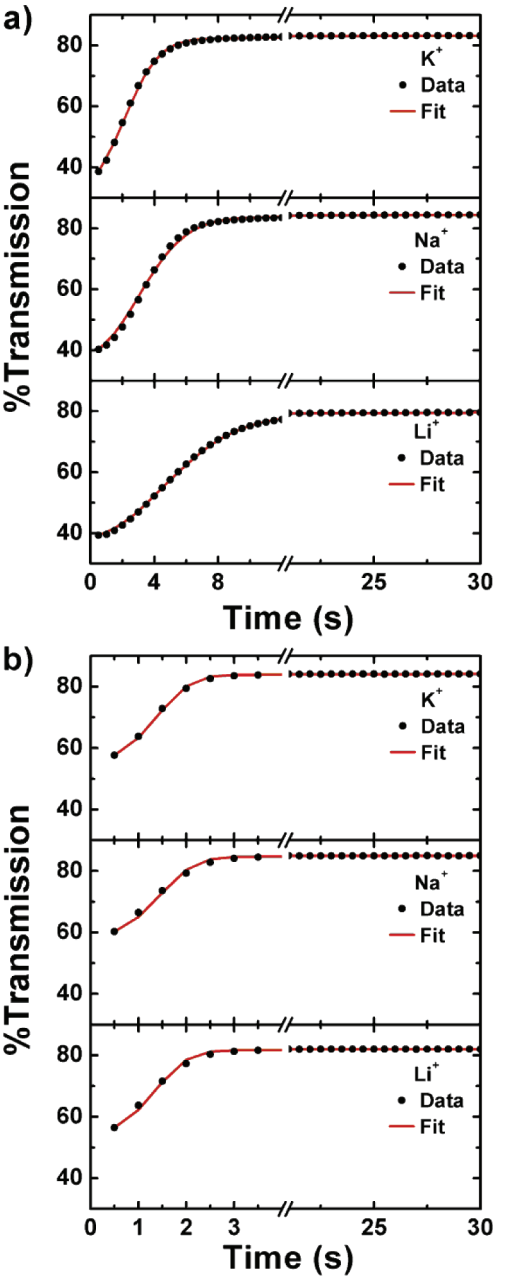

Figure 6. UV−vis transmission response of (a) as-spun and (b) DCA-treated PANI-PAAMPSA while undergoing transitions between the PB and ES oxidations state in 100 mM pH 5 acetate buffer solutions employing potassium (top), sodium (middle), and lithium (bottom) cations. Traces are reported (●) and fitted (red line) at the wavelength associated with maximum contrast.

Panels a and b in Figure 6 show the transmission response of as-spun and DCA-treated films, respectively, upon transitioning from PB to ES in each of the buffer solutions. The as-spun films exhibit a linear correlation between switching times and the hydrated cation size of the buffer solution; as the hydrated cation size increases from K^+ to Na^+ to Li^+, the time required to

dx.doi.org/10.1021/cm2023289 |*Chem. Mater.* 2011, 23, 4402–4409

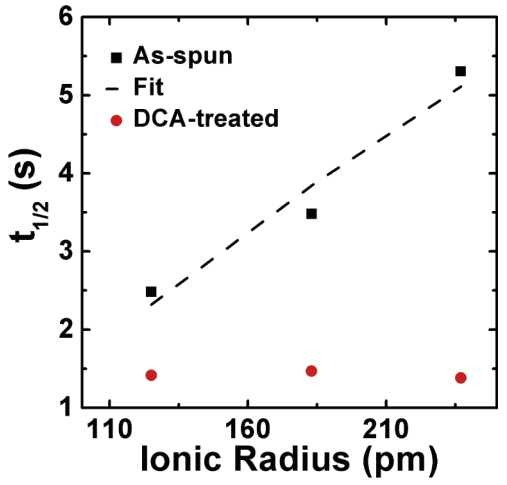

Figure 7. Extracted halftimes for PB to ES transitions in (■) as-spun and (red circle) DCA-treated PANI-PAAMPSA films as a function of the hydrated ionic radius of the acetate buffer solution's cation. The dashed line represents a linear fit for the as-spun films.

approach completion of the PB to ES transition increases from 6 to 8 to 12 s, respectively. Following DCA treatment, all films approach completion of the PB to ES transition within 3 s regardless of hydrated cation size. To more clearly illustrate the influence of the buffer's cation size, halftimes extracted from the stretched exponential portion of the fits depicted in Figure 6 are shown in Figure 7 as a function of hydrated cation radius.[39,40]

In consideration of Scheme 1 and the understanding that cations with larger radii possess poorer ionic conductivities,[40] we observe a slower electrochromic response rate with increases in the cation size. Smaller cations, alternatively, possess the mobility to more effectively traverse the internal complexities of the film, and consequently, permit faster oxidation of PANI from PB to ES. This effect, however, is unique to as-spun PANI-PAAMPSA films. For DCA-treated films, no discernible correlation was observed between PANI-PAAMPSA's electrochromic performance and the hydrated radius of the electrolytic solution's cation. The decrease in switching time and elimination of correlation with cation size following DCA treatment demonstrates the influence of internal mesoscale structure in electrochromic switching. We speculate that densification of the film following the collapse and homogenization of PANI-PAAMPSA particles reduces internal tortuosity within the film, and thereby enhances electrochromic response rate.

■ CONCLUSIONS

We have shown how the mesoscopic structure of conducting polymer films can influence several aspects of electrochromic switching. By employing our ability to tune the structure of PANI-PAAMPSA, we have provided the first quantitative model that accurately describes transitions between each of the three oxidation states associated with PANI. Further, we have been able to correlate the stretched exponential portion of the model with the identity of the induced oxidation state, the structure of the film, and the nature of the electrolyte. Our results provide direct and quantitative evidence of the development of a percolating conduction pathway for transitions to the ES state, and for the first time, we have been able to attribute dimensionality to this percolation (and differences therein). In addition, our studies indicate that the kinetics associated with the development of this percolation pathway exhibit a direct correlation with the cation size of the electrolyte, thereby providing guidelines for selecting the appropriate buffer species a priori to enable rapid switching.

Reynolds and others have performed enormous amounts of work synthesizing libraries of electrochromic and polyelectrochromic polymers,[13] but complexities in structure does not allow easy decoupling of kinetic parameters. Accordingly, the electrochromic community has, until now, been poorly equipped to understand the influence of structure on film performance. Our ability to compare various films comprised of predetermined PANI-PAAMPSA particle sizes, and our ability to induce a uniform control comparison via DCA treatment, provides unique and important insight into this subject.

■ AUTHOR INFORMATION

Corresponding Author

*E-mail: jtarver@princeton.edu; lloo@princeton.edu.

Author Contributions

The manuscript was written through contributions of all authors. All authors have given approval to the final version of the manuscript.

■ ACKNOWLEDGMENT

This work was supported by the Beckman Foundation and the National Science Foundation through a CAREER Award (DMR-0735148) and a PIRE grant (PIRE-0730243). J.T. acknowledges funding from the NSF Graduate Research Fellowship and the NIST-ARRA Graduate Fellowship programs.

■ REFERENCES

(1) Mortimer, R. J.; Dyer, A. L.; Reynolds, J. R. *Displays* **2006**, *27*, 2–18.

(2) Wolf, J. F.; Miller, G. G.; Shacklette, L. W.; Elsenbaumer, R. L.; Baughman, R. H., Adjustable tint window with electrochromic conductive polymer. U.S. Patent 4 893 908, 1990; viewable via Google Patents.

(3) DeLongchamp, D. M.; Kastantin, M.; Hammond, P. T. *Chem. Mater.* **2003**, *15*, 1575–1586.

(4) Argun, A. A.; Aubert, P. H.; Thompson, B. C.; Schwendeman, I.; Gaupp, C. L.; Hwang, J.; Pinto, N. J.; Tanner, D. B.; MacDiarmid, A. G.; Reynolds, J. R. *Chem. Mater.* **2004**, *16*, 4401–4412.

(5) Lee, K. S.; Blanchet, G. B.; Gao, F.; Loo, Y.-L. *App. Phys. Lett.* **2005**, *86*, 074102.

(6) Mano, N.; Yoo, J. E.; Tarver, J.; Loo, Y.-L.; Heller, A. *J. Am. Chem. Soc.* **2007**, *129*, 7006–7007.

(7) Lee, K. S.; Smith, T. J.; Dickey, K. C.; Yoo, J. E.; Stevenson, K. J.; Loo, Y. L. *Adv. Funct. Mater.* **2006**, *16*, 2409–2414.

(8) Garnier, F.; Tourillon, G.; Gazard, M.; Dubois, J. C. *J. Electroanal. Chem. Interfacial Electrochem.* **1983**, *148*, 299–303.

(9) Bjorklund, R.; Andersson, S.; Allenmark, S.; Lundström, I. *Mol. Cryst. Liq. Cryst.* **1985**, *121*, 263–270.

(10) Sotzing, G. A.; Reddinger, J. L.; Katritzky, A. R.; Soloducho, J.; Musgrave, R.; Reynolds, J. R.; Steel, P. J. *Chem. Mater.* **1997**, *9*, 1578–1587.

(11) Sapp, S. A.; Sotzing, G. A.; Reynolds, J. R. *Chem. Mater.* **1998**, *10*, 2101–2108.

(12) Witker, D.; Reynolds, J. R. *Macromolecules* **2005**, *38*, 7636–7644.

(13) Beaujuge, P. M.; Reynolds, J. R. *Chem. Rev.* **2010**, *110*, 268–320.

(14) McManus, P. M.; Yang, S. C.; Cushman, R. J. *J. Chem. Soc., Chem. Commun.* **1985**, 1556–1557.

(15) Epstein, A. J.; Ginder, J. M.; Zuo, F.; Bigelow, R. W.; Woo, H. S.; Tanner, D. B.; Richter, A. F.; Huang, W. S.; MacDiarmid, A. G. *Synth. Met.* **1987**, *18*, 303–309.
(16) Cao, Y.; Smith, P.; Heeger, A. J. *Synth. Met.* **1992**, *48*, 91–97.
(17) Yang, Y.; Heeger, A. J. *App. Phys. Lett.* **1994**, *64*, 1245–1247.
(18) Lee, K.; Cho, S.; Heum Park, S.; Heeger, A. J.; Lee, C.-W.; Lee, S.-H. *Nature* **2006**, *441*, 65–68.
(19) Kobayashi, T.; Yoneyama, H.; Tamura, H. *J. Electroanal. Chem. Interfacial Electrochem.* **1984**, *161*, 419–423.
(20) Watanabe, A.; Mori, K.; Iwasaki, Y.; Nakamura, Y.; Niizuma, S. *Macromolecules* **1987**, *20*, 1793–1796.
(21) Gospodinova, N.; Terlemezyan, L. *Prog. Polym. Sci.* **1998**, *23*, 1443–1484.
(22) DeLongchamp, D. M.; Hammond, P. T. Electrochromic Polyaniline Films from Layer-by-Layer Assembly. In *Chromogenic Phenomena in Polymers*; American Chemical Society: Washington, D.C., 2004; Vol. 888, pp 18−33.
(23) Jia, P.; Argun, A. A.; Xu, J.; Xiong, S.; Ma, J.; Hammond, P. T.; Lu, X. *Chem. Mater.* **2010**, *22*, 6085–6091.
(24) Bartlett, P. N.; Wang, J. H. *J. Chem. Soc., Faraday Trans.* **1996**, *92*, 4137–4143.
(25) Hu, H.; Hechavarria, L.; Campos, J. *Solid State Ionics* **2003**, *161*, 165–172.
(26) Yoo, J. E.; Cross, J. L.; Bucholz, T. L.; Lee, K. S.; Espe, M. P.; Loo, Y.-L. *J. Mater. Chem.* **2007**, *17*, 1268–1275.
(27) Yoo, J. E.; Bucholz, T. L.; Jung, S.; Loo, Y.-L. *J. Mater. Chem.* **2008**, *18*, 3129–3135.
(28) Yoo, J. E.; Krekelberg, W. P.; Sun, Y.; Tarver, J. D.; Truskett, T. M.; Loo, Y.-L. *Chem. Mater.* **2009**, *21*, 1948–1954.
(29) Tarver, J.; Yoo, J. E.; Loo, Y.-L. *Chem. Mater.* **2010**, *22*, 2333–2340.
(30) Tarver, J.; Yoo, J. E.; Dennes, T. J.; Schwartz, J.; Loo, Y.-L. *Chem. Mater.* **2008**, *21*, 280–286.
(31) Yoo, J. E.; Lee, K. S.; Garcia, A.; Tarver, J.; Gomez, E. D.; Baldwin, K.; Sun, Y.; Meng, H.; Nguyen, T.-Q.; Loo, Y.-L. *Proc. Natl. Acad. Sci. U.S.A.* **2010**, *107*, 5712–5717.
(32) DeLongchamp, D. M.; Hammond, P. T. *Chem. Mater.* **2004**, *16*, 4799–4805.
(33) Zhao, L.; Zhao, L.; Xu, Y.; Qiu, T.; Zhi, L.; Shi, G. *Electrochim. Acta* **2009**, *55*, 491–497.
(34) Hanson, E. L.; Schwartz, J.; Nickel, B.; Koch, N.; Danisman, M. F. *J. Am. Chem. Soc.* **2003**, *125*, 16074–16080.
(35) Greczynski, G.; Kugler, Th.; Salanek, W. R. *Thin Solid Films* **1999**, *354*, 129–135.
(36) Avrami, M. *J. Chem. Phys.* **1939**, *7*, 1103–1112.
(37) Avrami, M. *J. Chem. Phys.* **1940**, *8*, 212–224.
(38) Avrami, M. *J. Chem. Phys.* **1941**, *9*, 177–184.
(39) Itaya, K.; Ataka, T.; Toshima, S. *J. Am. Chem. Soc.* **1982**, *104*, 4767–4772.
(40) Ohno, H.; Yamazaki, H. *Solid State Ionics* **1993**, *59*, 217–222.